Journal of Hazardous Materials 431 (2022) 128556

Contents lists available at ScienceDirect

Journal of Hazardous Materials

journal homepage: www.elsevier.com/locate/jhazmat

Research Paper

Multivariable optimization of activated carbon production from microwave pyrolysis of brewery wastes - Application in the removal of antibiotics from water

Érika M.L. Sousa [a], Marta Otero [b,e], Luciana S. Rocha [a], María V. Gil [c], Paula Ferreira [d], Valdemar I. Esteves [a], Vânia Calisto [a,*]

[a] Department of Chemistry and CESAM, University of Aveiro, 3810-193 Aveiro, Portugal
[b] Department of Environment and Planning and CESAM, University of Aveiro, 3810-193 Aveiro, Portugal
[c] Instituto de Ciencia y Tecnología del Carbono, INCAR-CSIC, Francisco Pintado Fe 26, 33011 Oviedo, Spain
[d] Department of Materials and Ceramic Engineering and CICECO, University of Aveiro, 3810-193 Aveiro, Portugal
[e] Department of Applied Chemistry and Physics, Universidad de León, Campus de Vegazana, 24071 León, Spain

HIGHLIGHTS

- A fractional factorial design was applied to produce brewery waste-based materials.
- Optimization allowed for high reduction in pyrolysis time and activating agents.
- Highly porous activated carbons (AC) were obtained, with S_{BET} up to 1405 m^2 g^{-1}.
- Produced AC were tested for the removal of 3 antibiotics from water.
- Fast equilibrium times and high adsorption capacities were achieved.

GRAPHICAL ABSTRACT

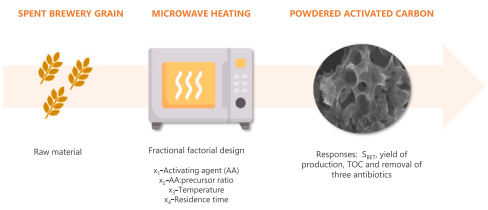

ARTICLE INFO

Editor: Arturo J. Hernandez-Maldonado

Keywords:
Spent brewery grain
Waste-based adsorbents
Fractional factorial design
Pharmaceuticals
Water treatment

ABSTRACT

This study aimed at optimizing the one-step chemical activation and microwave pyrolysis of an agro-industrial waste to obtain a microporous activated carbon (AC) with superior textural and adsorptive properties by a fast, low-reagent and low-energy process. Spent brewery grains were used as precursor, and the antibiotics sulfamethoxazole (SMX), trimethoprim (TMP) and ciprofloxacin (CIP) were considered as target adsorbates. A fractional factorial design was applied to evaluate the effect of the main factors affecting the preparation of AC (activating agent, activating agent:precursor ratio, pyrolysis temperature and residence time) on relevant responses. Under optimized conditions (K_2CO_3 activation, pyrolysis at 800 °C during 20 min and a K_2CO_3:precursor ratio of 1:2), a microporous AC with specific surface area of 1405 m^2 g^{-1} and large adsorption of target antibiotics (82–94%) was obtained and selected for further studies. Equilibrium times up to 60 min and maximum Langmuir adsorption capacities of 859 μmol g^{-1} (SMX), 790 μmol g^{-1} (TMP) and 621 μmol g^{-1} (CIP) were obtained. The excellent textural and adsorptive properties of the selected material were achieved with a very fast pyrolysis and low load of activating agent, highlighting the importance of optimization studies to decrease the environmental and economic impact of waste-based AC.

* Corresponding author.
E-mail address: vania.calisto@ua.pt (V. Calisto).

https://doi.org/10.1016/j.jhazmat.2022.128556
Received 6 December 2021; Received in revised form 17 February 2022; Accepted 21 February 2022
Available online 23 February 2022

1. Introduction

Antibiotics are a vast class of pharmaceuticals and have been considered a relevant group of emerging microcontaminants. Even detected at low concentrations (commonly from ng to μg L^{-1}), these compounds are able to induce chronic and acute adverse effects on human and animals, along with the development of bacterial resistance (Chaturvedi et al., 2021; Kovalakova et al., 2020). Recently, to fight antimicrobial-resistant bacteria, the European Union created the European One Health Action Plan (European Commission. Directorate General for Health and Food Safety., 2018). Also included antibiotics in the watch lists of substances for Union-wide monitoring that have been set in the field of water policy pursuant to Directive 2008/105/EC (the last watch list was established by Decision (EU) 2020/1161). Considering antibiotics wide consumption, their ubiquitous presence in environmental waters and the possible associated risks, the development of sustainable and effective treatment technologies for their removal from water is urgent in order to mitigate their entrance into the environment and therefore to reduce their impact on water quality and human/-animal health (Kovalakova et al., 2020).

Over the past few decades, adsorption has been described as an efficient and versatile method with low initial investment and no by-products generation in treated waters, resulting in the effective removal of pharmaceuticals from water, including antibiotics, even at low concentrations (Malakootian et al., 2019; Silva et al., 2018; Turk Sekulic et al., 2019). To date, a large variety of adsorbents has been proposed for this goal, including carbon-based materials (from which activated carbons (AC) are the most representative), clays, metal oxides, polymeric resins and chitosan (Carrales-Alvarado et al., 2014; Li et al., 2019; Oliveira et al., 2018; Premarathna et al., 2019; Tsukamoto et al., 2009; Uivarosi, 2013; Wu et al., 2016). Carbonaceous materials such as coal, wood, lignite and coconut shells are usually used to produce commercially available AC (Alahabadi et al., 2020; Brazil et al., 2020; Jackowski et al., 2020; Li et al., 2020). Alternatively, agro-industrial by-products, such as lignocellulosic wastes, can provide valid and sustainable sources of AC. This option is particularly attractive since the annual harvesting and processing of various crops produce considerable quantities of wastes. Also, the use of such environmentally friendly precursors can reduce the challenges involved with solid waste management while reducing the cost of feedstock for AC production. AC can be produced through physical or chemical activation of a variety of wastes combined with thermal decomposition (carbonization) (Danish and Ahmad, 2018). Traditionally, the carbonization step consists of a pyrolysis conversion using conventional heating, which generally requires long operation time and high temperature, being a high energy demanding process and thus, resulting in an increased production cost (Alslaibi et al., 2013). Microwave-assisted pyrolysis is a potential alternative to overcome these limitations due to the rapid, uniform heating, which results in shorter production times and lower energy consumption (Saucier et al., 2015). AC produced by this alternative heating have been used for the adsorption of different pollutants, and recent studies have shown that antibiotics may be successfully removed from water by AC prepared from microwave-assisted pyrolysis of various waste biomass, such as seed pods, giant reed, paper mill sludge and almond shells (Ahmed and Theydan, 2014; Chayid and Ahmed, 2015; Sousa et al., 2021; Zbair et al., 2018).

Spent brewery grain (SBG) is a by-product of the brewing industry consisting of the remains from the barley malt after the mashing process, which represents 85% of the total by-products. SBG is mainly composed of polysaccharides (hemicellulose and cellulose) and also lignin, proteins and lipids (de Araújo et al., 2020a; Sousa et al., 2020). The high content in lignocellulosic fibers makes it an attractive precursor for the production of AC (de Araújo et al., 2020b). The utilization of SBG as precursor in the production of AC for the adsorptive removal of pollutants from water has already been reported in the literature (Jackowski et al., 2020). In the specific case of pharmaceutical pollutants, Sousa et al. (2020) and de de Araújo et al. (2020a) reported the adsorption of carbamazepine and acetaminophen (paracetamol), respectively, by AC produced through conventional pyrolysis of SBG. Sousa et al. (2020) reported high values of the specific surface area (S_{BET}), ranging from 1090 to 1120 m^2 g^{-1}. However, to the best of the authors' knowledge, there are no studies on the adsorptive removal of antibiotics from water using SBG-based AC, neither on the production of AC from SBG through microwave assisted pyrolysis.

In the above described context, the aim of this work was to produce, for the first time, AC by one-step chemical activation and microwave-assisted pyrolysis of SBG, to be subsequently applied in the removal of antibiotics from water. Sulfamethoxazole (SMX), trimethoprim (TMP) and ciprofloxacin (CIP) were selected as antibiotic models since they belong to different classes (sulfonamides, diaminopyrimidines and fluoroquinolones, respectively) and they were all included in the last published watch list (Decision (EU) 2020/1161). In order to optimize the multivariable production process using a controlled number of experiments, an experimental design was applied. A fractional factorial design (FFD) was used allowing to study the main effects of varying the considered production variables: nature of activating agent, activating agent:precursor ratio, pyrolysis temperature and pyrolysis residence time. The evaluated responses included the yield of production, S_{BET}, total organic carbon (TOC) and percentage of adsorption of the antibiotics SMX, TMP and CIP from water at specific conditions. After optimizing the production conditions, the resulting material was further characterized and applied in kinetic and equilibrium studies of adsorption of the referred antibiotics from ultrapure water.

2. Materials and methods

2.1. Reagents and chemicals

The antibiotics sulfamethoxazole (SMX, 99.0%, TCI), trimethoprim (TMP, 98.0%, Sigma-Aldrich) and ciprofloxacin (CIP, 98.0%, TCI) were used for adsorption tests, their physico-chemical properties being displayed within Supplementary Material (SM) in Table S1 and Fig. S1. Sodium hydroxide (NaOH, 99.3%, José Manuel Gomes dos Santos), potassium hydroxide (KOH, ≥86.0%, BCHM), potassium carbonate (K_2CO_3, 99.9%, AnalaR normapur) and phosphoric acid (H_3PO_4, 85.0%, Acros organics) were used as chemical activating agents for AC production, whereas hydrochloric acid (HCl, 37.0%, Honeywell FLUKA) was used for washing the pyrolyzed materials. For the quantification of antibiotics in aqueous samples by Micellar Electrokinetic Chromatography (MEKC) (as described in SM1), the separation buffer consisted of sodium tetraborate (Borax, ≥99.5%, Riedel-de Haën) and sodium dodecyl sulfate (SDS, 99.0%, Sigma Aldrich), while ethylvanillin (99.0%, Sigma-Aldrich) was used as internal standard. For capillary coating, hexadimethrine bromide (polybrene, ≥95.0%, Sigma–Aldrich), sodium chloride (NaCl, ≥99.5%, Fluka) and NaOH (99.3%, José Manuel Gomes dos Santos) were used. HCl (37.0%, Honeywell FLUKA), NaOH (99.3%, José Manuel Gomes dos Santos) and NaCl (≥99.5%, Fluka) were used for the determination of the point of zero charge. All the solutions were prepared in ultrapure water obtained from a PURELAB Flex 4 system (Elga, Veolia).

2.2. Production of carbon adsorbents

SBG resulting from the production of pilsener beer was collected from the Brewery *Faustino Microcervejeira, Lda* (Aveiro, Portugal) and used as precursor for AC productions. After collection, SBG was dried at room temperature for several days, followed by 24 h at 100 °C in an oven. Then, SBG was roughly grinded with a blade mill (until obtaining a rough SBG powder with particles with size up to ~ 1 mm) and stored until use. Proximate analyses of this precursor were determined in a previous work described by Sousa et al. (2020) and are depicted in Table S2, as Supplementary Material (SM2). In a preliminary analysis,

alkaline activating agents as KOH, NaOH, K_2CO_3 and the acidic agent H_3PO_4 were tested for AC production, using an activating agent:precursor ratio of 1:1 (*w*:*w*) in all cases. The impregnation was carried out using an activating agent solution that was mixed with SBG, generating a slurry that was subsequently sonicated for 1 h in an ultrasonic bath and dried at room temperature for several days. Then, impregnated SBG was pyrolyzed under N_2 atmosphere in a CEM Phoenix™ AirWave microwave furnace, where the impregnated precursor was heated at a rate of 15 °C min^{-1} up to 800 °C, applying a residence time of 20 min after the maximum temperature was reached. The used microwave furnace is equipped with a programmable temperature controller and a temperature sensor, which allows for programming the heating time (min) desired to achieve the final pyrolysis temperature, thus enabling the definition of the referred heating rate. Next, a preliminary assessment on the adsorptive performance of the resulting materials in the removal of antibiotics SMX, TMP and CIP from water was done. Obtained results, which are depicted as SM, allowed to identify the KOH and K_2CO_3 as the most adequate activating agents to be subsequently applied in the FFD.

For the FFD, for each production condition, 30 g of raw material was impregnated with KOH or K_2CO_3 at different activating agent:precursor ratios (1:1; 1:2 or 1:5). Accordingly, aqueous solutions of KOH or K_2CO_3 with the concentrations of 0.30 g mL^{-1}, 0.15 g mL^{-1} and 0.06 g mL^{-1} were used for achieving activating agent:precursor ratios of 1:1, 1:2 and 1:5 (*w*/*w*), respectively. The impregnated materials were heated at a rate of 15 °C min^{-1} up to 600, 700 or 800 °C, keeping these temperatures constant for 10, 20 or 30 min.

All the produced AC were washed step with 1.2 M HCl for 1 h (for ashes removal), followed by distilled water (until neutral pH of the washing leachate), and dried overnight at 50 °C. Finally, the AC were crushed and sieved to obtain a particle size $\leq$ 180 μm.

2.3. Fractional factorial design

A FFD was applied to select the optimal conditions to produce AC from SBG using microwave-assisted pyrolysis. A FFD is usually used to reduce the number of experiments when many factors need to be evaluated. The selected factors and the evaluated responses will be presented and discussed in the following sub-Section.

2.3.1. Factors

Four factors were selected, namely, activating agent (x_1); activating agent: precursor ratio (x_2); temperature (x_3) and residence time (x_4). These variables were chosen based on a previous work (Sousa et al., 2020, 2021) and preliminary experiments. The optimization process was performed using a FFD with mixed levels (three factors at three levels and one factor at two levels), resulting in $3^{3-1} \times 2$ experiments. Overall, eighteen AC were obtained and named AC1 to AC18. The experimental domain of each factor was delimited by three or two levels as described in Table 1. The lower, medium and high levels were coded as − 1, 0 and + 1, respectively. The mathematical model associated to the FFD design is a polynomial model (Alimohammadi et al., 2016) described by Eq. (1):

$$Y = b_0 + \sum_{i=1}^{k} b_i x_i + \sum_{\substack{1 \le i \le n-1 \\ i+1 < j \le n}} b_{ij} x_i x_j + \sum_{i=1}^{k} b_i x_i^2 \quad (1)$$

where Y is the response of interest (yield of production (Y_1), specific surface area (Y_2), total organic carbon (Y_3) and percentage of adsorption (Y_4)), b_0 is the average value, b_i is the main effect of the factor i, b_{ij} is the interaction effect between factors i and j, and x_i and x_j are the factors.

2.3.2. Responses

The evaluated responses were the yield of production (%), S_{BET}, TOC and percentage of adsorption of SMX, TMP and CIP from water at specific conditions.

2.3.2.1. Yield of production (%). The yield of production (%) was calculated as described in Eq. (2) for all the produced carbon materials:

$$Yield\ of\ production(\%) = \frac{w_f}{w_i} x100\% \quad (2)$$

where w_f (g) is the final mass of AC (after pyrolysis, washing and drying) and w_i (g) is the initial mass of the dried precursor.

2.3.2.2. Specific surface area. The S_{BET} of the produced materials was obtained using a Micromeritics Instrument, Gemini VII 2380 at 77 K. The degassing of the samples was conducted at 120 °C. Nitrogen adsorption-desorption experiments were then carried out through liquid nitrogen at -196 °C. The relative pressure of 0.99 was used to estimate the total pore volume (V_p). Brunauer-Emmet-Teller equation (Brunauer et al., 1938) was used to calculate S_{BET} in a relative pressure range between 0.001 and 0.1. Microporosity (W_0) was determined by Dubinin-Astakov equation (Dubinin, 1975) to the lower relative pressure zone of the nitrogen adsorption isotherm. The average micropore width (L) was measured by means of the Stoeckli–Ballerini equation (Stoeckli and Ballerini, 1991). The average pore diameter parameter (D) was calculated by Eq. (3) (Calisto et al., 2014):

$$D = 2x\frac{V}{S_{BET}} \quad (3)$$

2.3.2.3. Total organic carbon. For all the materials, total carbon (TC) and inorganic carbon (IC) quantification were determined in a TOC analyser (TOC-V_{CPH} Shimadzu) connected to a solid sample module (SSM-5000A, Japan). TOC was calculated by the difference between TC and IC values. All analyses were performed in triplicate.

2.3.2.4. Adsorption experiments. Batch adsorption experiments were carried out to determine the percentage of adsorption of the antibiotics under study onto the eighteen produced AC. Single solutions of the antibiotics SMX, TMP or CIP were prepared in ultrapure water with an initial concentration of 20 μmol L^{-1}. Adsorption experiments were conducted in 50 mL polypropylene falcon tubes by putting in contact 1.0 mg of each AC with 40 mL of the antibiotics aqueous solutions (corresponding to an adsorbent final dosage of 25 mg L^{-1}). The tubes were then shaken at 80 *rpm* in an overhead shaker (Heidolph, Reax 2) at controlled temperature of 25 ± 0.1 °C, during 24 h. After that, solutions were filtered through 0.22 μm PVDF filters (Whatman) and analysed for the remaining concentration of antibiotic in the aqueous phase by Micellar Electrokinetic Chromatography using UV-Vis detection at 200 nm (as described in detail in SM1). Control experiments consisting of antibiotic solutions without adsorbent were performed simultaneously and used as reference for the calculation of adsorption percentages, using Eq. (4):

$$Adsorption(\%) = \frac{C_i - C_f}{C_i} x100 \quad (4)$$

Table 1
Factors and levels used in factional factorial design for preparation of activated carbons from spent brewery grain.

Factors	Levels		
	-1	0	+ 1
Activating agent (x_1)	KOH	–	K_2CO_3
Activating agent: precursor ratio (*w*/*w*) (x_2)	1:1	1:2	1:5
Temperature (°C) (x_3)	600	700	800
Residence time (min) (x_4)	10	20	30

where C_i (μmol L^{-1}) is the concentration of antibiotic in the corresponding control experiments (from now on, taken as the initial antibiotic concentration) and C_f (μmol L^{-1}) is the remaining antibiotic concentration in the liquid phase at the end of the adsorption experiment with each AC. All experiments were carried out in triplicate.

2.3.3. Data treatment

The FFD together with the response surface methodology (RSM) were used to evaluate the effect of each factor on each response. The models were validated using analysis of variance (ANOVA) and the correlation coefficient (R^2). The *p*-values were used to check the significance of each factor (x_1, x_2, x_3 and x_4) for the selected responses (confidence level of 95%). Significant and non-significant factors were represented by *p*-values ≤ 0.05 and *p*-values > 0.05, respectively. Also, a principal component analysis (PCA) was applied for pattern recognition within the produced AC dataset since it can highlight both the similarities and differences between them. The STATISTICA 10 software (StatSoft, Tulsa, OK, USA) was used for the statistical analysis of the results.

2.4. Physical and chemical characterization of the selected material

Based on the results obtained in Section 2.3, one of the produced AC was selected for further characterization, namely by scanning electron microscopy (SEM), X-ray photoelectron spectroscopy (XPS) and point of zero charge (PZC). A detailed description of the procedures used in these analyses can be found in SM4.

2.5. Kinetic and equilibrium adsorption studies

According with results obtained in Section 2.3, one AC was selected and evaluated in terms of kinetic and equilibrium studies. The description of the procedures is reported in the next sub-sections.

2.5.1. Kinetic experiments and modeling

To evaluate the time needed to attain equilibrium, single solutions with 20 μmol L^{-1} of each antibiotic under study were shaken with the selected AC in ultrapure water. The adsorption kinetic experiments were conducted as described in Section 2.3.2.4 with the adjustments next described. These experiments were conducted in 150 mL polypropylene falcon tubes, where 100 mL of antibiotic aqueous solutions were shaken together with 1.5 mg of the selected AC (at final adsorbent dosage of 15 mg L^{-1}), during eight time intervals (t) between 5 and 240 min.

The adsorbed concentration of each pharmaceutical onto the selected AC at a time t (min), q_t (μmol g^{-1}), was calculated using Eq. (5):

$$q_t = \frac{(C_i - C_f) \times V}{m} \quad (5)$$

where C_i (μmol L^{-1}) is the initial antibiotic concentration (control solution), C_f is the final antibiotic concentration (μmol L^{-1}) after shaking during a time t (min), V is the volume of the solution (L) and m is the mass (mg) of adsorbent.

The pseudo-first order (Lagergren, 1898) and pseudo-second order (Ho et al., 2000) models, which integrated forms with the boundary conditions of $q_t = 0$ at t = 0 and $q_t = q_t$ at t = t are respectively represented by Eqs. (6) and (7), were evaluated to describe the obtained data.

$$q_t = q_e\left(1 - e^{-k_1 t}\right) \quad (6)$$

$$q_t = \frac{q_e^2 k_2 t}{1 + q_e k_2 t} \quad (7)$$

where q_e is the amount of antibiotic per AC unit of mass at equilibrium (μmol g^{-1}), k_1 is the pseudo-first order rate constant (min^{-1}) and k_2 is the pseudo-second order rate constant (g μmol min^{-1}). Note that q_t is represented in μmol g^{-1} to allow a better comparison of results obtained for the three pharmaceuticals under study, considering that the adsorption occurs at the molecular level and the studied antibiotics have different molecular weights. Fittings to the described kinetic models were obtained by non-linear regression analysis using GraphPad Prism version 8.0.1.

2.5.2. Equilibrium experiments and modeling

Equilibrium adsorption experiments were carried out as referred in the previous section, but at different doses of the selected AC, namely between 10 and 45 mg L^{-1} for experiments with CIP, and 12.5–40 mg L^{-1} for SMX and TMP. According to the results obtained in Section 2.5.1, the solutions were shaken during 240 min to guarantee equilibrium.

Experimental data were described using the non-linear models of Langmuir (homogeneous monolayer adsorption) (Langmuir, 1918) and Freundlich isotherms (heterogeneous adsorption of the solute onto the adsorbent surface) (Freundlich, 1907), represented by Eqs. (8) and (9), respectively:

$$q_e = \frac{q_m K_L C_e}{1 + K_L C_e} \quad (8)$$

$$q_e = K_F \times C_e^{\frac{1}{N}} \quad (9)$$

where q_e (μmol g^{-1}) represents the concentration of solute adsorbed at equilibrium, q_m (μmol g^{-1}) is the Langmuir maximum adsorption capacity at the equilibrium, K_L (L μmol^{-1}) is the Langmuir equilibrium constant, C_e (μmol L^{-1}) is the concentration of each antibiotic at equilibrium in the solution, K_F (μmol g^{-1}(μmol $L^{-1})^{-N}$) is the Freundlich equilibrium constant, and N is the degree of non-linearity. Note that q_e is represented in μmol g^{-1} to allow a better comparison of results obtained for the three pharmaceuticals under study, as referred above for q_t in Eqs. 6 and 7.

The software GraphPad Prism version 8.0.1 was used to perform the non-linear regression analysis and to determine the fitted equilibrium parameters for the Langmuir and Freundlich isotherm models.

3. Results and discussion

3.1. Fractional factorial design: responses

The levels of each studied factor to produce the eighteen AC and the corresponding responses assessed by the FFD (namely yield of production (%), S_{BET}, TOC and % adsorption for each antibiotic) are shown in Table 2.

Regarding the yield of production (%) determined by Eq. 2, the results indicate a decrease in the yield with increasing temperature (from 600 to 800 °C). The highest yields (up to 14%) were obtained for the pyrolysis temperature of 600 °C. The lowest product yields (between 1% and 8%) were obtained for KOH or K_2CO_3-based AC (activating agents selected according to preliminary tests described in SM3) at the two highest temperatures studied (700 and 800 °C), which would be due to the high loss of volatile organic matter originated by the reaction with alkaline activating agents (Sousa et al., 2020). These relatively low yields should be related to the large content in volatiles (75.75 *wt*%) in opposition to the small fixed carbon content (only 19.3%) (Table S2 SM), which resulted in high volatile release during pyrolysis and high generation of porosity. Also, it should be noted that the high volatile content points to the possibility of energy reuse through pyrolysis, which can significantly reduce energy costs. The yield of production also appeared to be influenced by the activating agent:precursor ratio, with the highest yields (11% and 14%) obtained for AC produced with an activating agent:precursor ratio of 1:5. Similar yields to those obtained in the present work were also reported by Mussatto et al. (2010) when using the same precursor to produce AC by conventional pyrolysis and H_3PO_4 as activating agent. These authors also observed a strong

Table 2
Factors and corresponding levels used in the fractional factorial design for the preparation of activated carbons together with the obtained responses.

AC	Factors				Responses					
	x_1	x_2	x_3	x_4	Yield (%)	S_{BET} (m^2 g^{-1})	TOC*	Ads SMX (%)*	Ads TMP (%)*	Ads CIP (%)*
1	KOH	1:1	600	20	6	1047	74 ± 1	52 ± 6	48 ± 5	50 ± 6
2	KOH	1:1	700	20	4	1066	67 ± 1	71 ± 2	60 ± 2	75 ± 3
3	KOH	1:1	800	30	5	1240	71 ± 1	88 ± 2	77 ± 4	92 ± 4
4	KOH	1:2	600	30	6	1072	74 ± 2	41 ± 5	51 ± 3	58 ± 5
5	KOH	1:2	700	20	3	1011	66 ± 1	47 ± 4	51 ± 3	67 ± 3
6	KOH	1:2	800	10	1	1171	57 ± 1	72 ± 6	64 ± 5	90 ± 4
7	KOH	1:5	600	30	14	648	69 ± 1	5 ± 4	8 ± 3	17 ± 9
8	KOH	1:5	700	10	10	728	70 ± 1	11 ± 6	15 ± 4	22 ± 9
9	KOH	1:5	800	10	7	795	71 ± 1	17 ± 6	22 ± 4	31 ± 4
10	K_2CO_3	1:1	600	10	10	948	72.3 ± 0.4	33 ± 6	24 ± 5	16 ± 4
11	K_2CO_3	1:1	700	10	8	854	67 ± 1	40 ± 6	25 ± 5	38 ± 5
12	K_2CO_3	1:1	800	30	7	1138	67 ± 1	75 ± 5	70 ± 2	72 ± 2
13	K_2CO_3	1:2	600	10	11	659	71 ± 1	11 ± 7	7 ± 4	10 ± 7
14	K_2CO_3	1:2	700	30	8	1212	58.6 ± 0.4	58 ± 6	63 ± 3	78 ± 4
15	K_2CO_3	1:2	800	20	8	1405	65 ± 1	82 ± 4	84 ± 2	94 ± 1
16	K_2CO_3	1:5	600	20	11	533	69 ± 1	8 ± 5	10 ± 3	25 ± 6
17	K_2CO_3	1:5	700	30	7	782	60 ± 1	28 ± 6	31 ± 4	44 ± 5
18	K_2CO_3	1:5	800	20	3	1124	67 ± 1	44 ± 4	36 ± 3	48 ± 7

* Mean value ± standard deviation (n = 3).

decrease in the yield of production with increasing temperature depending on the activating agent:precursor ratio. Also, according to Guo and Rockstraw (2006), the yield of production can be significantly affected by the origin of the lignocellulose, which can impact its molecular structure.

In what concerns to the textural properties of the AC, the S_{BET} values, shown in Table 2 and Fig. 1a, evidenced an increasing tendency as a function of temperature. The S_{BET} of the AC produced at 600 °C ranged between 533 and 1047 m^2 g^{-1}, while that of the AC produced at 800 °C ranged between 795 and 1405 m^2 g^{-1}. An increase in the total pore volume (V_p), micropore volume (W_0), average micropore width (L) and average pore diameter (D) can also be observed with increasing temperature from 600° to 800°C (see Table S4 in SM). Other authors have reported that a more extensive carbonization has been evidenced by an increase in S_{BET} and total pore volume resulting from higher pyrolysis temperature (Lee and Park, 2010; Moulefera et al., 2020). Regarding the pyrolysis residence time (10, 20 and 30 min), no obvious effects in the S_{BET} values or in the determined textural properties were observed. The same behavior was reported by Sousa et al. (2021) using paper mill sludge as raw material and microwave pyrolysis, under similar production conditions. Overall, KOH-AC and K_2CO_3-AC showed very similar textural properties under the same production conditions. Also, when analysing the results obtained under pyrolysis at 800 °C and with K_2CO_3, the S_{BET} did not suffer large variations by increasing the ratio of activating agent:precursor from 1:1–1:5, indicating that the complete carbonization and high porosity development might have been attained even at relative low activating agent proportions. It is noteworthy that a ratio of 1:5 activating agent:precursor was used in this work, while ratios of 1:0.5 and 1:0.25 are usually reported in the literature (Aldred et al., 2014; Lillo-Ródenas et al., 2007). Moreover, the AC with the highest S_{BET} obtained in this study was produced with 1:2 activating agent:precursor ratio, which is not the highest ratio of activating agent: precursor studied. The results obtained in the present work are very satisfactory when compared with other studies in literature using SBG as AC precursor. For example, in the work by Osman et al. (2020), SBG was activated with H_3PO_4 and subjected to a 500 °C carbonization for 30 min, and the resulting AC was activated with KOH (KOH:precursor ratio of ~1:0.3) and subjected to a second carbonization at 500 °C for 30 min. The high amount of activating agent with two successive impregnations and a two-step conventional pyrolysis resulted in an AC with a S_{BET} of only 497 m^2 g^{-1}. In a different study, Sousa et al. (2020)) used conventional pyrolysis (800 °C for 150 min) to produce AC from KOH-impregnated SBG and achieved S_{BET} values ranging from 1090 to 1120 m^2 g^{-1}, applying an activating agent:precursor ratio of 1:1. The materials here produced under the same pyrolysis temperature (800 °C), using KOH as activating agent (AC 1–6) at the same or lower ratios but with significantly shorter pyrolysis residence times (between 6 and 18 times shorter), showed equal or superior results in terms of S_{BET} than those obtained by Sousa et al. (2020).

In what concerns to the TOC of the produced materials, high TOC percentages, ranging between 57 ± 1 and 74 ± 1%, were obtained for all AC, corroborating the effective carbonization of the raw material,

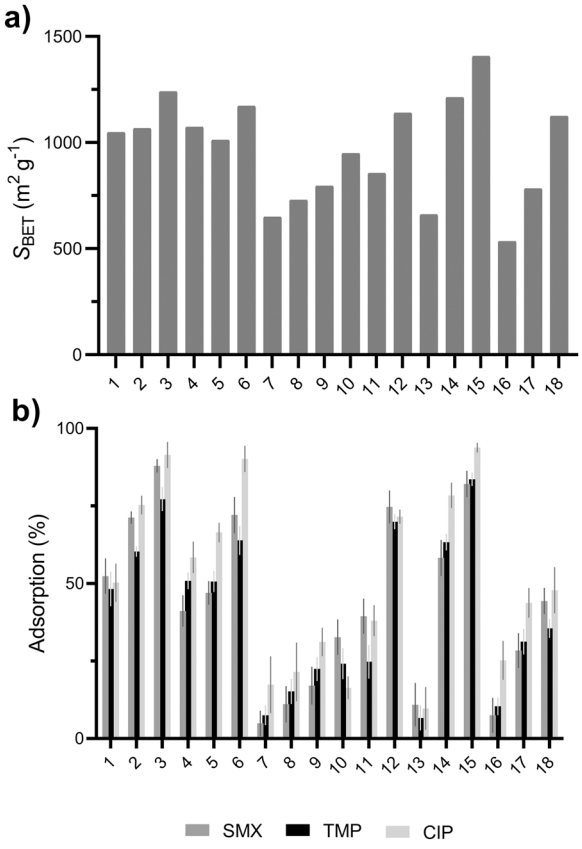

Fig. 1. a) S_{BET} results and **b)** adsorption percentage for SMX, TMP and CIP of produced AC numbered from 1 to 18. Error bars are displayed for each AC.

which is in line with the high values of S_{BET}. Although it was not included as a response in the factorial design, it is noteworthy that all the produced AC presented IC percentages below 0.14% (see SM5 Table S5), suggesting an efficient acid washing in the removal of ash and other inorganic matter naturally present in the precursor or arising from microwave pyrolysis.

Results of the adsorption tests for the evaluation of the removal efficiency of SMX, TMP and CIP are depicted in Table 2 and Fig. 1b. These results show an increase in the percentage of adsorption with the temperature of production for all the studied pharmaceuticals, in accordance with the results obtained for S_{BET}. Furthermore, it is evident that under pyrolysis at 800 °C adsorption percentages barely varied when increasing the activating agent:precursor ratio from 1:1 to 1:2. Nevertheless, for the activating agent:precursor ratio of 1:5 (AC 7–9 and AC 16–18), a significant decrease in adsorption percentage was clearly observed, indicating that such accentuated decrease in the amount of activating agent had a clear impact in the adsorption efficiency of the resulting materials. Overall, and in accordance with S_{BET}, the best adsorptive performance was obtained by AC15 (S_{BET} of 1405 $m^2 g^{-1}$) for all the antibiotics under study, attaining adsorption percentages ranging between 82 ± 4 and 94 ± 1%.

3.2. Analysis of variance

To statistically evaluate which factors significantly influence the studied responses, an analysis of variance was performed, and the obtained results are described in Table 3.

The *p*-values obtained at 95% confidence level indicate that the type of activating agent (x_1) was the only factor with no influence on any of the considered responses ($p > 0.05$ for all the responses). The results are in accordance with the first analysis and discussion of the results in Section 3.1, since both activating agents (KOH and K_2CO_3) present similar behavior for the evaluated responses. The other factors (activating agent:precursor ratio (x_2), temperature (x_3) and residence time (x_4)) significantly influenced several responses, as indicated by *p*-values < 0.05.

The influence of the activating agent:precursor ratio (x_2) on S_{BET} (Jaria et al., 2018; Örkün et al., 2012; Sousa et al., 2021) and adsorptive performance (El Maguana et al., 2018; Jaria et al., 2018; Sousa et al., 2021) has also been evidenced by other studies in the literature. In the present study, the temperature (x_3) influenced all the responses evaluated. The important role of temperature is in agreement with some previous studies, which refer to temperature as the key parameter affecting numerous properties of carbon adsorbents (Calisto et al., 2014; Jaria et al., 2018; Örkün et al., 2012; Sousa et al., 2021). The studied levels of pyrolysis residence time (x_4) also influenced the adsorption results. Considering that both activating agents did not influence the responses and comparing the AC produced under the same conditions of temperature and activating agent:precursor ratio, it is possible to observe an increase in the adsorption percentage with the residence time. For example, comparing AC1 with AC10, both produced at 600 °C but using 20 and 10 min of pyrolysis residence time, respectively, significant differences in the adsorption percentage for the three antibiotics can be observed. The same behavior can be observed when other AC are compared including for 1:2 or 1:5 activating agent:precursor ratio, such as AC4 and AC13 or AC8 and AC17. Overall, the statistical analysis showed the temperature (x_3) as the main factor influencing all the evaluated responses, followed by the activating agent:precursor ratio (x_2).

3.3. Response surface methodology

Considering the above results, the response surfaces concerning the influence of temperature and the activating agent:precursor ratio on the considered responses were plotted and are presented in Fig. 2.

Analysing the results depicted in Fig. 2, there is no set of ideal and consensual conditions for all the studied responses simultaneously. As example, in Fig. 2a high yields were obtained for low temperatures, in opposition to S_{BET} (Fig. 2b) and the adsorption of the three studied antibiotics (Fig. 2d, e and f), which were clearly enhanced by the increase in temperature. The optimization evidences that, in a general way, 1 and 0.5 are the most convenient ratios of activating agent:precursor (x_2), and 800 °C is the most favorable pyrolysis temperature (x_3).

3.4. Principal component analysis

The biplot of the PCA analysis, which is represented in Fig. 3, shows that PCA 1 and PCA 2 account for 74.9% and 14.6% of the variance,

Table 3
Analyzes of variance (ANOVA) obtained for each evaluated response at 95% confidence level.

Responses	Factors[a]	Sum of square	df	Mean of square	F-test	*p*-value[b]
Yield (%)	x_1	1.21×10^1	1	1.21×10^1	1.64	0.2
	x_2	1.34×10^1	2	6.68×10	0.90	0.4
	x_3	7.42×10^1	2	3.71×10^1	5.03	**0.03**
	x_4	9.64×10	2	4.82×10	0.65	0.5
S_{BET} ($m^2 g^{-1}$)	x_1	8.27×10^2	1	8.27×10^2	0.05	0.8
	x_2	3.66×10^5	2	1.83×10^5	10.91	**0.003**
	x_3	3.28×10^5	2	1.64×10^5	9.78	**0.004**
	x_4	1.08×10^5	2	5.40×10^4	3.22	0.08
TOC (%)	x_1	2.46×10^5	1	2.46×10^1	1.44	0.2
	x_2	5.91×10^1	2	2.95×10^1	1.74	0.2
	x_3	1.42×10^5	2	7.11×10^1	4.18	**0.05**
	x_4	1.02×10^1	2	5.09×10	0.30	0.7
Adsorption sulfamethoxazole (%)	x_1	3.89×10^1	1	3.89×10^1	0.53	0.5
	x_2	5.64×10^3	2	2.82×10^3	38.53	**0.00002**
	x_3	4.36×10^3	2	2.18×10^3	29.81	**0.00006**
	x_4	1.52×10^3	2	7.59×10^2	10.37	**0.004**
Adsorption trimethoprim (%)	x_1	1.21×10^2	1	1.21×10^2	1.53	0.2
	x_2	4.00×10^3	2	2.00×10^3	25.43	**0.0001**
	x_3	3.50×10^3	2	1.75×10^3	22.22	**0.0002**
	x_4	2.10×10^3	2	1.05×10^3	13.37	**0.001**
Adsorption ciprofloxacin (%)	x_1	3.33×10^2	1	3.33×10^2	2.92	0.1
	x_2	3.97×10^3	2	1.98×10^3	17.36	**0.0006**
	x_3	5.21×10^3	2	2.60×10^3	22.77	**0.0002**
	x_4	2.60×10^3	2	1.30×10^3	11.37	**0.003**

[a] Activating agent (x_1); activating agent: precursor (x_2); temperature (x_3); residence time (x_4).
[b] The bold *p*-values indicate a significant effect of the factor on the response.

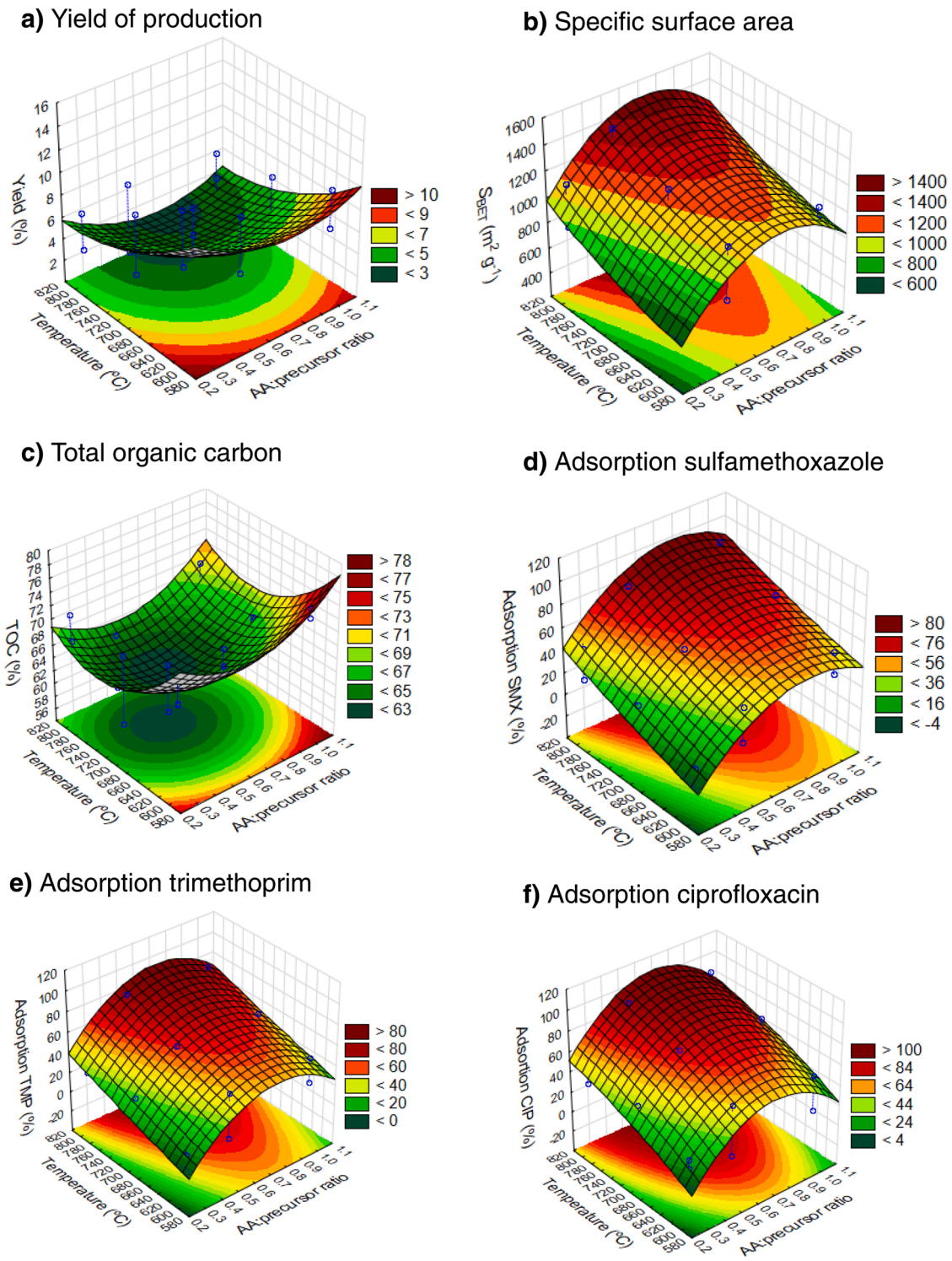

Fig. 2. Response surfaces concerning temperature vs activating agent (AA):precursor ratio for the **a)** yield of production (%), **b)** specific surface area (S_{BET}), **c)** total organic carbon (TOC), and adsorption of **d)** sulfamethoxazole, **e)** trimethoprim and **f)** ciprofloxacin.

respectively.

The results clearly show two distinct groups of materials. The first group is constituted by AC resulting from processes with high production yield (between 11% and 14%), such as AC7, AC13 and AC16, but with low S_{BET} and antibiotics adsorption percentages. Another very interesting insight is that, overall, for the eight AC grouped with the highest yields, five are impregnated with K_2CO_3, evidencing that impregnation with K_2CO_3 results in AC with improved yields. The second group is characterized by AC with the highest values of S_{BET} (above 1011 $m^2\ g^{-1}$) and the highest percentages of antibiotics adsorption (ranging between 47 ± 4% (AC5) and 94 ± 1% (AC15)). Amongst these materials, AC3 (KOH; 1:1; 800 °C for 30 min) and AC15 (K_2CO_3; 1:2, 800 °C for 20 min) stand out as the ones that globally combine the highest S_{BET} and adsorption percentages for the three considered antibiotics. Taking into account their similarities concerning performance and textural properties and considering that AC15 requires softer

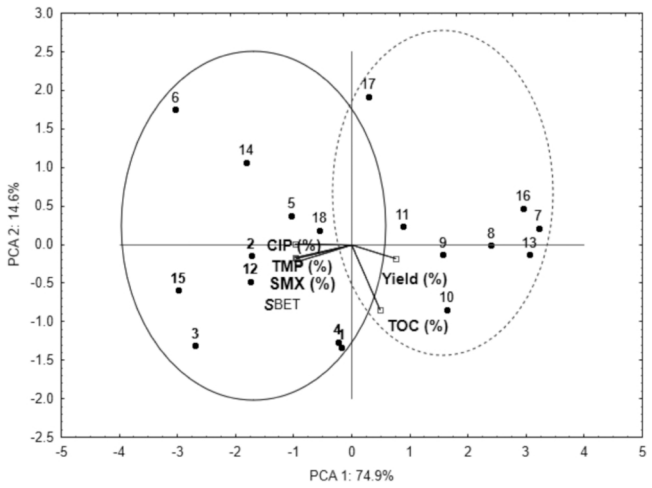

Fig. 3. Principal component analysis (PCA).

production conditions (half of the activating agent amount and shorter pyrolysis time when compared to AC3), which has a direct influence in the economic and environmental impacts (see a laboratorial scale cost assessment in section SM6), it was selected for further characterization and evaluation of the adsorptive performance.

3.5. Physical and chemical characterization of the selected activated carbon

The morphological features of AC15 together with images of the SBG precursor (for comparison purposes) were obtained by SEM micrographs, which are displayed in Fig. 4.

The surface of the SBG used as precursor appears to be homogeneous and smooth, without the presence of an evident porous structure. On the other hand, AC15 presents a more cratered and fractured surface with a well-developed porous structure, which is favorable for an effective adsorbent-adsorbate interaction. Overall, the porous structure is in accordance with the high values obtained for the total pore volume (V_p of 0.67 $cm^3\ g^{-1}$) and microporous volume (W_0 of 0.64 $cm^3\ g^{-1}$) and the large S_{BET} (1405 $m^2\ g^{-1}$) (see Table S4 in SM5).

XPS analysis was used to obtain additional information of functional groups present on surface of AC15. The overall spectra is presented in Fig. S2 SM and show the presence of two main peaks, ascribed to C 1s and O 1s core levels. Other small peaks, namely Si 2p and N 1s, were also found. Analysing the relative atomic abundance in the surface of the material, the XPS data showed contents of 78% of carbon and 14% of oxygen. The C 1s spectra present four main peaks at binding energy between 284.4 and 290.6 eV. By deconvolution of C 1s region, it is detected the presence of: graphitic Csp^2 (284.4 eV peak 1) (Nielsen et al., 2014); functional groups (C – C sp^3, C – O, N,H): phenolic, alcoholic, etheric carbon (285.2 eV peak 2) (Nielsen et al., 2014; Velo-Gala et al., 2014); C – O single bond, ether and alcohol groups (286.5 eV peak 3) (Velo-Gala et al., 2014); C – O:carbonyl, quinones and ketones (287.5 eV peak 4); and finally, the presence of π – π * transition in C (290.6 eV peak 5) (Lingamdinne et al., 2017). Regarding the deconvoluted O 1s XPS spectra of AC15 shown in Fig. S2 in SM, four peaks were observed with binding energies between 532.7 and 535.3 eV. These binding energies were assigned to CO (532.7ev, peak 1), C – O – H (532.6 eV, peak 2) and – COOH or COOR (533.8 eV, peak 3) functional groups, and to physiosorbed water (533.3 eV, peak 4) (Lee et al., 2016).

Concerning PZC, the net surface charge of AC15 is zero at pH 5. Considering that the surface charge of the AC depends on the solution pH and its PZC, for aqueous solutions with pH below the PZC the surface of AC is predominantly positively charged, while for pH above PZC the surface is predominantly negatively charged. The slightly acidic PZC may be attributed to the chemical activation using K_2CO_3. In the work reported by Sousa et al. (2020), neutral or slightly basic PZC were obtained for AC prepared by pyrolysis and chemical activation of SBG but with the alkaline agent KOH instead of K_2CO_3.

3.6. Kinetic and equilibrium performance of the selected activated carbon

3.6.1. Kinetic studies and modeling

The graphical representation of kinetic experimental data (q_t (μmol g^{-1}) *vs* time (min)) is depicted in Fig. 5, along with fitted results to the considered mathematical models (Eqs. (6) and (7), Section 2.5.1); the corresponding kinetic parameters being presented in Table 4.

According to the results depicted in Fig. 5 and Table 4, it can be observed that SMX, TMP and CIP are quickly adsorbed onto AC15 in the first minutes of contact, reaching the equilibrium after approximately 60 min. To the best of the authors' knowledge, there are no published studies on the adsorption of antibiotics onto carbon materials produced from brewery wastes. However, the same equilibrium time was reported by Sousa et al. (2021) for the adsorption of SMX, under identical experimental conditions, but using AC produced through the microwave pyrolysis of paper mill sludge. In another study reported by Silva et al. (2019), also using AC derived from paper mill sludge, the same equilibrium time was reported for the adsorption of SMX under similar experimental conditions, but using a slightly higher adsorbent dose

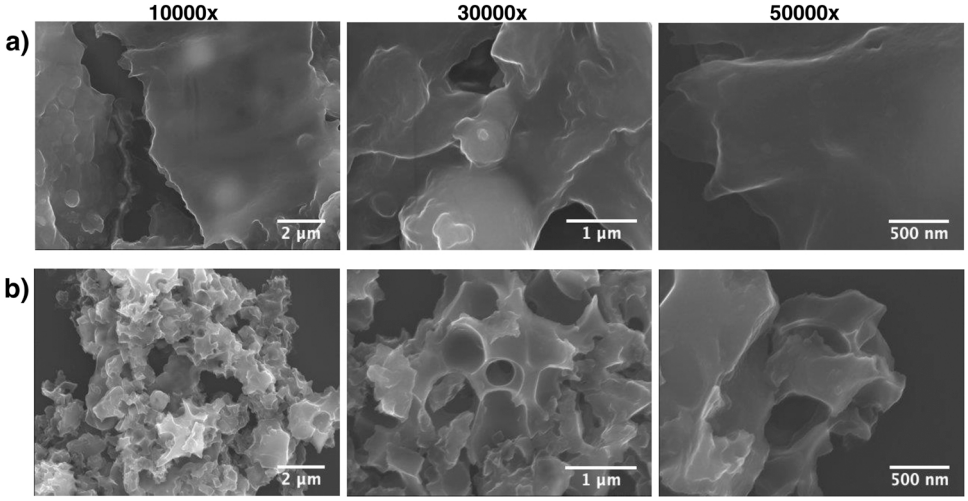

Fig. 4. SEM micrographs of the **a)** SBG precursor and **b)** AC15, at different magnifications.

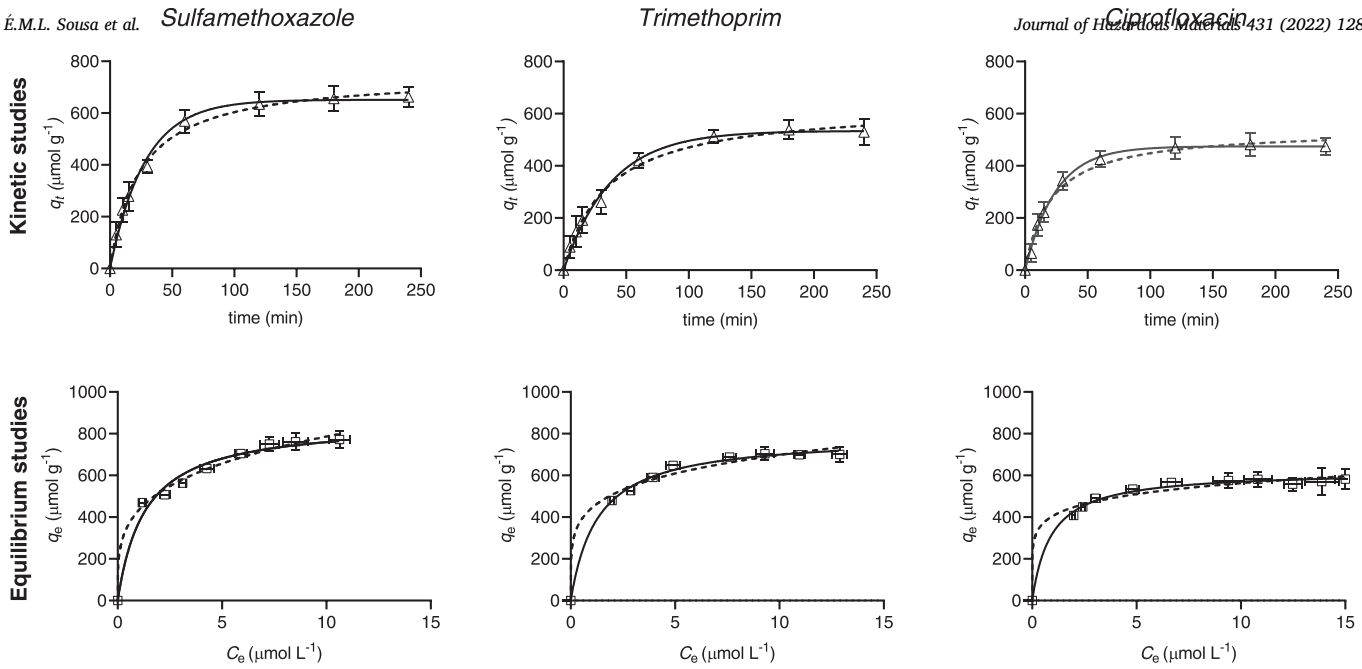

Fig. 5. Kinetic and equilibrium experimental data obtained for the adsorption of SMX, TMP and CIP onto AC15. Fittings to the kinetic reaction models of pseudo-first (–) and pseudo-second (–) order and to the equilibrium isotherm models of Langmuir (–) and Freundlich (–) are represented together with the corresponding experimental results. Experimental conditions: 20 μmol L^{-1} of SMX, TMP and CIP (single solutions), material dose of 15 mg L^{-1} (kinetic) and 10–45 mg L^{-1} (equilibrium), stirring (80 rpm) at 25.0 °C ± 0.1 °C. Note: Error bars stand for standard deviations, n = 3.

Table 4
Fitting parameters of kinetic and equilibrium models concerning the adsorption of the antibiotics sulfamethoxazole, trimethoprim and ciprofloxacin onto AC15.

		Sulfamethoxazole	Trimethoprim	Ciprofloxacin
Kinetic models				
Pseudo-first order	k_1 (min^{-1})	(3.6 ± 0.2) x10^{-2}	(2.6 ± 0.2) x10^{-2}	(4.1 ± 0.2) x10^{-2}
	q_e (μmol g^{-1})*	651 ± 12	534 ± 12	475 ± 6
	q_e (mg g^{-1})*	165 ± 8	155 ± 3	157 ± 2
	R^2	0.994	0.993	0.997
	S_{yx}	20.88	18.91	11.23
Pseudo-second order	k_2 (g μmol^{-1} min^{-1})	(6 ± 5) x10^{-5}	(5 ± 6) x10^{-5}	(9 ± 1) x10^{-5}
	q_e (μmol g^{-1})*	748 ± 16	633 ± 21	541 ± 18
	q_e (mg g^{-1})*	189 ± 4	184 ± 6	79 ± 6
	R^2	0.995	0.992	0.989
	S_{yx}	18.07	19.43	21.66
Isotherm models				
Langmuir	q_m (μmol g^{-1})*	859 ± 36	790 ± 14	621 ± 10
	q_m (mg g^{-1})*	217 ± 9	229 ± 4	206 ± 3
	K_L (L μmol^{-1})	0.8 ± 0.1	0.8 ± 0.1	1.1 ± 0.1
	R^2	0.982	0.996	0.994
	S_{yx}	34.6	14.6	14.2
Freundlich	K_F (μmol g^{-1}(μmol L^{-1})$^{-N}$)	433 ± 15	443 ± 23	406 ± 18
	N	3.8 ± 0.3	5.1 ± 0.6	7 ± 1
	R^2	0.993	0.987	0.981
	S_{yx}	21.4	27.0	24.6

* q_e and q_m values were presented both in μmol g^{-1} and mg g^{-1} to facilitate the comparison of the results with literature.

(20 mg L^{-1}). For TMP, according to the information found in the literature, long equilibrium times above 10 h were reported by Cheng et al. (2014) using 100 μmol L^{-1} of TMP and an adsorbent dose (AC from chicken feathers) of 0.2 g L^{-1}. Similarly to the present study, equilibrium times of ~60 min were reported by Zhang et al. (2017) for the removal of CIP by AC from desilicated rice husk. However, the experimental conditions used in that study, namely adsorbent dose (0.3 g L^{-1}) and CIP initial concentration (1207 μmol L^{-1}), were not directly comparable to those used in the present work. The relative short equilibrium time, even for the adsorption of antibiotics with different physico-chemical properties such as the considered here, is a major positive characteristic of the here produced AC.

As it may be seen in Table 4, both fittings to the pseudo-first and pseudo-second order models presented R^2 above 0.98. Due to their simple analytical solutions and good fitting abilities, these are the most frequently used models for the description of adsorption kinetic data, notwithstanding their empirical nature (Hu et al., 2021; Rodrigues and Silva, 2016). Both the pseudo-first and pseudo-second are reaction models, which assume that the adsorption rate is ruled by the adsorption reactions occurring at the solid/liquid interface and that the difference between the actual and the equilibrium surface concentration of the adsorbate is the driving force for adsorption (Rudzinski and Plazinski, 2007). In any case, analysing the correlation coefficient R^2, and the standard deviation of the residuals (S_{yx}) in Table 4, it can be said that the pseudo-first order model was the most suitable to describe the adsorption kinetics for the three antibiotics under study. Hence, physisorption

Table 5
Literature data on the adsorption of sulfamethoxazole, trimethoprim and ciprofloxacin from water by commercial and waste-based AC.

Antibiotic	Adsorbent	Production conditions (pyrolysis type, temperature, residence time, activating agent: precursor ratio)	S_{BET} (m^2 g^{-1})	Experimental conditions (antibiotic initial concentration, adsorbent dose; temperature; pH)	q_m (μmol g^{-1})*	q_m (mg g^{-1})*	Reference
Sulfamethoxazole	Commercial AC	–	851	79 μmol L^{-1}; 0.02–0.8 g L^{-1}; 25 °C; pH not adjusted	731	185	(Çalışkan and Göktürk, 2010)
	AC from primary paper mill sludge	Conventional, 800 °C, 150 min, 1:1	1627	20 μmol L^{-1}; 0.008–0.05 g L^{-1}; 25 °C; pH not adjusted	766	194	(Silva et al., 2019)
	Functionalized biochar	Conventional, 600 °C, 120 min, 1:2	1.1	2–197 μmol L^{-1}; 0.01 g L^{-1}; 21 °C; pH not adjusted	319	81	(Ahmed et al., 2017)
	AC from bleached paper pulp	Conventional, 800 °C, 150 min, 1:1	965	20 μmol L^{-1}; 0.03–0.30 g L^{-1}; 25 °C; pH not adjusted	434	110	(Oliveira et al., 2018)
	AC from walnut shell	Conventional, 900 °C, 120 min, 1:1	934	2–158 μmol L^{-1}; 0.01 g L^{-1}; 30 °C; pH 5.5	367	93	(Teixeira et al., 2019)
	AC from paper mill sludge	Microwave, 800 °C, 20 min, 1:5	1196	20 μmol L^{-1}; 0.01–0.05 g L^{-1}; 25 °C; pH not adjusted	857	217	(Sousa et al., 2021)
	AC from almond shell	Microwave, 700 °C, 120 min, 1:0.1	1274	20–395 μmol L^{-1}; 0.01 g L^{-1}; 25 °C; pH 5	1362	345	(Zbair et al., 2018)
	AC from spent brewery grain (AC15)	Microwave, 800 °C, 20 min, 1:2	1405	20 μmol L^{-1}; 0.012–0.04 g L^{-1}; 25 °C; pH not adjusted	859	217	**This work**
Trimethoprim	Commercial AC	–	882	172 μmol L^{-1}; 0.1–0.5 g L^{-1}; 25 °C; pH not adjusted	888	258	(Kim et al., 2010)
	Commercial GAC	–	1112	172 μmol L^{-1}; 0.1–2 g L^{-1}; 25 °C; pH not adjusted	1120	325	(Kim et al., 2010)
	Commercial AC	–	745	20–197 μmol L^{-1}; 0.1 g L^{-1}; room temperature; pH 6	434	126	(Berges et al., 2021)
	AC from common reed	Conventional, 750 °C, 60 min, 1:0.5	1534	300–7000 μmol L^{-1}; 0.2 g L^{-1}; 25 °C; pH 7.3	1285	373	(Liu et al., 2015)
	AC from lotus stalk	Conventional, 500 °C, 60 min, 1:0.4	1114	100–300 μmol L^{-1}; 0.2 g L^{-1}; 25 °C; pH not adjusted	1148	333	(Liu et al., 2012)
	AC from chicken feathers	Conventional, 600 °C, 50 min, 1:0.5	589	100 μmol L^{-1}; 0.2 g L^{-1}; 20 °C; pH not adjusted	565	164	(Cheng et al., 2014)
	AC from spent brewery grain (AC15)	Microwave, 800 °C, 20 min, 1:2	1405	20 μmol L^{-1}; 0.01–0.04 g L^{-1}; 25 °C; pH not adjusted	790	229	**This work**
Ciprofloxacin	Commercial AC	–	1237	0–75 μmol L^{-1}; 0.05 g L^{-1}; 25 °C; pH not adjusted	697	231	(Carabineiro et al., 2012)
	Commercial AC	–	974	0–75 μmol L^{-1}; 0.05 g L^{-1}; 25 °C; pH not adjusted	712	236	(Carabineiro et al., 2011)
	AC from desilicated rice husk	Conventional, 950 °C, 30 min, 1:0.3	1020	0–604 μmol L^{-1}; 0.4 g L^{-1}; 25 °C; pH 7.9	1394	462	(Zhang et al., 2017)
	AC from bamboo waste	Conventional, 850 °C, 30 min, 1:0.3	2237	25–118 μmol L^{-1}; 0.5 g L^{-1}; room temperature; pH not adjusted	327	108	(Wang et al., 2015)
	AC from giant reed	Microwave, 700 °C, 15 min, ~1:2	1568	604–3622 μmol L^{-1}; 1 g L^{-1}; 25 °C; pH 6	1312	435	(Sun et al., 2014)
	AC from spent brewery grain (AC15)	Microwave, 800 °C, 20 min, 1:2	1405	20 μmol L^{-1}; 0.01–0.045 g L^{-1}; 25 °C; pH not adjusted	621	206	**This work**

* For comparison purposes, Langmuir maximum adsorption capacities (q_m) values were presented in μmol L^{-1} and mg g^{-1}.

is probably the process underneath the adsorbate uptake onto AC15 since the pseudo-first order model is known to fail in the description of more complex chemisorption processes (with longer equilibrium times and usually described by the pseudo-second order kinetics model) (Agbovi and Wilson, 2021). As for the k_1, the adsorption kinetic rates determined for the three antibiotics were in the same order of magnitude and corroborate their similar and relative fast uptake shown in Fig. 5.

3.6.2. Equilibrium studies and modeling

As it may be seen in Fig. 5 and Table 4, experimental data on the adsorption of SMX, TMP and CIP were well described by both Langmuir and Freundlich models, with satisfactory correlation coefficients ($R^2 \geq 0.98$). Overall, the Langmuir model, which is valid for monolayer adsorption and assumes that adsorption sites are identical and homogeneous (Akhtar et al., 2011; Langmuir, 1918; Sun et al., 2014), exhibited higher R^2 values and lower S_{yx}, based on this, the referred fitting was considered to the subsequent discussion. Maximum adsorption capacities achieved by AC15 were 856 ± 36 μmol g^{-1}, 790 ± 14 μmol g^{-1} and 621 ± 10 μmol g^{-1} for SMX, TMP and CIP, respectively. A statistical comparison of these data (t-test, at 95% confidence level (Miller and Miller, 2005)) revealed that there are no significant differences for adsorption of SMX and TMP ($T_{cal}(0.1) < T_{tab}(3.18)$). Yet, the maximum adsorption capacity (in μmol g^{-1}) towards CIP is significantly lower than the ones for SMX and TMP. Analysing the pK_a and the corresponding speciation of each pharmaceutical (see Table S1 and Fig. S1 in SM) at the working pH (ultrapure water with pH ~ 5.5 (not adjusted)), it can be stated that CIP is present in a mixture of its positive and neutral (zwitterionic) form, SMX in a mixture of negative and neutral species, while TMP is mostly positively charged. In this scenario, if the electrostatic interactions were the ones ruling the adsorption process (and considering that the surface of AC15 is predominantly negative due to its PCZ of 5, according to Section 3.5), it would be expected that AC15 presented the highest adsorption capacity towards TMP. Under the tested conditions, this tendency was not verified, evidencing those electrostatic interactions might not be the ruling phenomena. A closer analysis to other physico-chemical properties of the 3 pharmaceuticals (Table S1, in SM) indicates that CIP is the one with the highest water solubility (S_w) and the lowest octanol-water partition coefficient (log K_{ow}), revealing its higher tendency to remain in the aqueous phase in comparison to the other 2 pharmaceuticals. As showed by Calisto et al. (2015), who evaluated 14 different adsorption systems (2 AC and 7 pharmaceuticals), log K_{ow} and S_w are amongst the properties of the pharmaceuticals with major influence on their adsorptive uptake by AC, observing a positive correlation of log K_{ow} and negative correlation of S_w with the maximum adsorption capacities. This evidence is in line with the tendency observed in this work. Also, in what concerns the influence of non-electrostatic interactions (which are also known to be particularly important in adsorption phenomena), literature studies using carbon-based materials indicated a decrease in adsorption capacities at acidic pH for CIP, reporting that the presence of interactions that can increase the adsorption capacity, such hydrophobic interactions (Bizi and El Bachra, 2020; Shang et al., 2016), and namely π-π interactions (Bizi and El Bachra, 2020; Carabineiro et al., 2011; García-Reyes et al., 2021), may be inhibited at lower pH. All these studies are in agreement with the results reported in this work.

For comparison purposes, Table 5 summarizes the relevant information on the properties (S_{BET}) and adsorption capacity (q_m) towards SMX, TMP and CIP by different commercial and waste-based adsorbents in the literature, together with their production conditions.

As it can be seen in Table 5, it is important to highlight that, even when produced under short residence time and low activating agent: precursor ratio, higher S_{BET} (1405 m^2 g^{-1}) was obtained for AC15 when compared to the majority of the depicted commercial AC. Furthermore, it is important to highlight that most waste-based AC reported in the literature were produced under higher residence times and higher ratios of activating agents than those used for the production of AC15. Moreover, even applying a residence time of only 20 min and an activating agent: precursor ratio of 1:2, the S_{BET} of AC15 was similar or higher than that for most of the reported waste-based AC produced by conventional or microwave pyrolysis from several wastes. Comparing all the AC obtained at 1:2 activating agent:precursor ratio (Table 5), AC15 has substantially superior or comparable S_{BET} values (Ahmed et al., 2017; Sun et al., 2014). Regarding q_m, in most cases, comparable or even higher values were obtained for AC15 than for commercial AC. Yet, the comparison of q_m obtained from different studies are not straightforward and any conclusions taken for such comparisons should be prudent. In fact, it should be noted that the higher adsorption reported in the literature for waste-based AC, for instance the AC produced from almond shell (Zbair et al., 2018), lotus stalk (Liu et al., 2012) and giant reed (Sun et al., 2014), applied to SMX, TMP and CIP, respectively, were obtained under quite different experimental conditions (adsorbent dose, initial antibiotic concentration temperature and pH) compared to those reported in the present study, making a direct comparison difficult. Indeed, it is noteworthy that the majority of studies presenting higher q_m than those here reported were carried out using larger concentrations of pharmaceuticals and/or larger doses of the materials under study. However, under very similar experimental conditions, as it is the case of the studies concerning the removal of SMX by AC from paper mill sludge produced by conventional (Silva et al., 2019) and microwave (Sousa et al., 2021) pyrolysis, comparable or even higher q_m were obtained for AC15.

3.6.3. Future work

The high potential and versatility demonstrated by the selected AC15 produced by microwave pyrolysis proved the necessity of carrying out kinetics and equilibrium studies to evaluate the performance in a real effluent. Furthermore, future developments of this work will include:

i) Study of the pH effect and evaluation of the adsorptive performance under competitive conditions considering mixed antibiotic solutions;
ii) Thermodynamic studies to investigate the adsorption mechanisms;
iii) Regeneration studies by microwave to allow reusing the materials and increase their lifetime, delaying end-of-life disposal.

4. Conclusions

The production of AC for antibiotics removal from water using brewery wastes as precursor and microwave pyrolysis (instead of conventional) was optimized through a FFD with mixed levels to study the effects of four factors (nature of activating agent, activating agent:precursor ratio, pyrolysis temperature and residence time) on six selected responses (yield of production, S_{BET}, TOC and adsorptive removal of SMX, TMP and CIP). The pyrolysis temperature showed the most significant effect, and this factor directly influenced all the evaluated responses. The optimized AC (AC15), which was obtained under pyrolysis at 800 °C during 20 min and applying K_2CO_3:precursor ratio of 1:2, exhibited a well-microporous structure, a S_{BET} value of 1405 m^2 g^{-1} and remarkable adsorptive removals (84–92%) for the considered antibiotics. Further studies with AC15 revealed that the kinetic experimental data were adequately described by pseudo-first order model and the adsorption equilibrium time for the three antibiotics was approximately 60 min. The equilibrium isotherms were adequately described by the Langmuir model, with maximum monolayer adsorption capacities of 859 μmol g^{-1}, 790 μmol g^{-1} and 621 μmol g^{-1} for SMX, TMP and CIP, respectively. The FFD optimization allowed for the production of an AC with outstanding properties and adsorptive performance by minimizing the consumption of activating agent and energy (short pyrolysis time using microwave heating) to values well below those used in the literature. Such findings highlight the importance of structured experimental designs in the optimization of AC production and reduction of the associated economic and environmental impacts.

CRediT authorship contribution statement

Érika M.L. Sousa: Investigation, Formal analysis, Writing - original draft. **Marta Otero:** Conceptualization, Writing - review & editing. **Luciana S. Rocha:** Conceptualization, Writing - review & editing. **María V. Gil:** Investigation. **Paula Ferreira:** Conceptualization, Supervision. **Valdemar I. Esteves:** Conceptualization, Supervision. **Vânia Calisto:** Conceptualization, Supervision, Funding acquisition, Writing - review & editing.

Declaration of Competing Interest

The authors declare that they have no known competing financial interests or personal relationships that could have appeared to influence the work reported in this paper.

Acknowledgments

This work was developed within the scope of the project CICECO - Aveiro Institute of Materials (UIDB/50011/2020 & UIDP/50011/2020). We acknowledge financial support to CESAM by FCT/MCTES (UIDP/50017/2020+UIDB/50017/2020+LA/P/0094/2020), through national funds. Érika M.L. Sousa thanks to Fundaç ão para a Ciência e Tecnologia (FCT) for her PhD grant (2020.05390. BD). Paula Ferreira is thankful to FCT for the Investigator Program (IF/00300/2015). María V. Gil acknowledges support from a Ramón y Cajal grant (RYC-2017-21937) of the Spanish government and the Spanish State Research Agency, co-financed by the European Social Fund (ESF).

Novelty statement

This study describes the production of highly efficient carbon adsorbents from brewery wastes and their application in the effective removal of antibiotics from water. A microwave-based thermal conversion was optimized achieving a one-step, fast and low-reagent process, decoupling the production of materials with excellent textural and adsorptive properties from processes with limited sustainability.

The described research gives a step forward in establishing microwave technology as an excellent greener alternative to conventional thermal treatments. This manuscript constitutes a significant contribution towards the development of materials for the effective removal of hazardous microcontaminants from water, without relegating the materials' sustainability to a secondary plan.

Appendix A. Supporting information

Supplementary data associated with this article can be found in the online version at doi:10.1016/j.jhazmat.2022.128556.

References

Agbovi, H.K., Wilson, L.D., 2021. Adsorption processes in biopolymer systems: fundamentals to practical applications. Nat. Polym. Green. Adsorbents Water Treat. 1–51. https://doi.org/10.1016/B978-0-12-820541-9.00011-9.

Ahmed, M.B., Zhou, J.L., Ngo, H.H., Guo, W., Johir, M.A.H., Sornalingam, K., 2017. Single and competitive sorption properties and mechanism of functionalized biochar for removing sulfonamide antibiotics from water. Chem. Eng. J. 311, 348–358. https://doi.org/10.1016/j.cej.2016.11.106.

Ahmed, M.J., Theydan, S.K., 2014. Fluoroquinolones antibiotics adsorption onto microporous activated carbon from lignocellulosic biomass by microwave pyrolysis. J. Taiwan Inst. Chem. Eng. 45, 219–226. https://doi.org/10.1016/j.jtice.2013.05.014.

Akhtar, J., Amin, N.S., Aris, A., 2011. Combined adsorption and catalytic ozonation for removal of sulfamethoxazole using Fe2O3/CeO2 loaded activated carbon. Chem. Eng. J. 170, 136–144. https://doi.org/10.1016/j.cej.2011.03.043.

Alahabadi, A., Singh, P., Raizada, P., Anastopoulos, I., Sivamani, S., Dotto, G.L., Landarani, M., Ivanets, A., Kyzas, G.Z., Hosseini-Bandegharaei, A., 2020. Activated carbon from wood wastes for the removal of uranium and thorium ions through modification with mineral acid. Colloids Surf. A Physicochem. Eng. Asp. 607, 125516 https://doi.org/10.1016/j.colsurfa.2020.125516.

Aldred, K.J., Kerns, R.J., Osheroff, N., 2014. Mechanism of quinolone action and resistance. Biochemistry 53, 1565–1574. https://doi.org/10.1021/bi5000564.

Alimohammadi, V., Sedighi, M., Jabbari, E., 2016. Response surface modeling and optimization of nitrate removal from aqueous solutions using magnetic multi-walled carbon nanotubes. J. Environ. Chem. Eng. 4, 4525–4535. https://doi.org/10.1016/j.jece.2016.10.017.

Alslaibi, T.M., Abustan, I., Ahmad, M.A., Foul, A.A., 2013. A review: production of activated carbon from agricultural byproducts via conventional and microwave heating. J. Chem. Technol. Biotechnol. 88, 1183–1190. https://doi.org/10.1002/jctb.4028.

Berges, J., Moles, S., Ormad, M.P., Mosteo, R., Gómez, J., 2021. Antibiotics removal from aquatic environments: adsorption of enrofloxacin, trimethoprim, sulfadiazine, and amoxicillin on vegetal powdered activated carbon. Environ. Sci. Pollut. Res. 28, 8442–8452. https://doi.org/10.1007/s11356-020-10972-0.

Bizi, M., El Bachra, F.E., 2020. Evaluation of the ciprofloxacin adsorption capacity of common industrial minerals and application to tap water treatment. Powder Technol. 362, 323–333. https://doi.org/10.1016/J.POWTEC.2019.11.047.

Brazil, T.R., Gonçalves, M., Junior, M.S.O., Rezende, M.C., 2020. A statistical approach to optimize the activated carbon production from Kraft lignin based on conventional and microwave processes. Microporous Mesoporous Mater. 308, 110485 https://doi.org/10.1016/j.micromeso.2020.110485.

Brunauer, S., Emmett, P.H., Teller, E., 1938. Adsorption of gases in multimolecular layers. J. Am. Chem. Soc. 60, 309–319. https://doi.org/10.1021/ja01269a023.

Calisto, V., Ferreira, C.I.A., Oliveira, J.A.B.P., Otero, M., Esteves, V.I., 2015. Adsorptive removal of pharmaceuticals from water by commercial and waste-based carbons. J. Environ. Manag. 152, 83–90. https://doi.org/10.1016/j.jenvman.2015.01.019.

Calisto, V., Ferreira, C.I.A., Santos, S.M., Gil, M.V., Otero, M., Esteves, V.I., 2014. Production of adsorbents by pyrolysis of paper mill sludge and application on the removal of citalopram from water. Bioresour. Technol. 166, 335–344. https://doi.org/10.1016/j.biortech.2014.05.047.

Çalışkan, E., Göktürk, S., 2010. Adsorption characteristics of sulfamethoxazole and metronidazole on activated carbon. Sep. Sci. Technol. 6395. https://doi.org/10.1080/01496390903409419.

Carabineiro, S.A.C., Thavorn-Amornsri, T., Pereira, M.F.R., Figueiredo, J.L., 2011. Adsorption of ciprofloxacin on surface-modified carbon materials. Water Res. 45, 4583–4591. https://doi.org/10.1016/j.watres.2011.06.008.

Carabineiro, S.A.C., Thavorn-amornsri, T., Pereira, M.F.R., Serp, P., Figueiredo, J.L., 2012. Comparison between activated carbon, carbon xerogel and carbon nanotubes for the adsorption of the antibiotic ciprofloxacin. Catal. Today 186, 29–34. https://doi.org/10.1016/j.cattod.2011.08.020.

Carrales-Alvarado, D.H., Ocampo-Pérez, R., Leyva-Ramos, R., Rivera-Utrilla, J., 2014. Removal of the antibiotic metronidazole by adsorption on various carbon materials from aqueous phase. J. Colloid Interface Sci. 436, 276–285. https://doi.org/10.1016/j.jcis.2014.08.023.

Chaturvedi, P., Shukla, P., Giri, B.S., Chowdhary, P., Chandra, R., Gupta, P., Pandey, A., 2021. Prevalence and hazardous impact of pharmaceutical and personal care products and antibiotics in environment: a review on emerging contaminants. Environ. Res. 194, 110664 https://doi.org/10.1016/j.envres.2020.110664.

Chayid, M.A., Ahmed, M.J., 2015. Amoxicillin adsorption on microwave prepared activated carbon from Arundo donax Linn: isotherms, kinetics, and thermodynamics studies. J. Environ. Chem. Eng. 3, 1592–1601. https://doi.org/10.1016/j.jece.2015.05.021.

Cheng, C., Zhang, J., Zhang, C., Liu, H., Liu, W., 2014. Preparation and characterization of charcoal from feathers and its application in trimethoprim adsorption. Desalin. Water Treat. 52, 5401–5412. https://doi.org/10.1080/19443994.2013.807477.

Danish, M., Ahmad, T., 2018. A review on utilization of wood biomass as a sustainable precursor for activated carbon production and application. Renew. Sustain. Energy Rev. 87, 1–21. https://doi.org/10.1016/j.rser.2018.02.003.

de Araújo, T.P., Quesada, H.B., Bergamasco, R., Vareschini, D.T., de Barros, M.A.S.D., 2020a. Activated hydrochar produced from brewer's spent grain and its application in the removal of acetaminophen. Bioresour. Technol. 310, 123399 https://doi.org/10.1016/j.biortech.2020.123399.

de Araújo, T.P., Tavares, F., de, O., Vareschini, D.T., Barros, M.A.S.D., 2020b. Biosorption mechanisms of cationic and anionic dyes in a low-cost residue from brewer's spent grain. Environ. Technol.) 0, 1–16. https://doi.org/10.1080/09593330.2020.1718217.

Dubinin, M.M., 1975. Physical Adsorption of Gases and Vapors in Micropores, Progress in Surface and Membrane Science. ACADEMIC PRESS, INC. https://doi.org/10.1016/b978-0-12-571809-7.50006-1.

El Maguana, Y., Elhadiri, N., Bouchdoug, M., Benchanaa, M., 2018. Study of the influence of some factors on the preparation of activated carbon from walnut cake using the fractional factorial design. J. Environ. Chem. Eng. 6, 1093–1099. https://doi.org/10.1016/j.jece.2018.01.023.

Freundlich, H., 1907. Über die Adsorption in Lösungen. Z. Phys. Chem. 57U, 385–470. https://doi.org/10.1515/zpch-1907-5723.

García-Reyes, C.B., Salazar-Rábago, J.J., Sánchez-Polo, M., Loredo-Cancino, M., Leyva-Ramos, R., 2021. Ciprofloxacin, ranitidine, and chlorphenamine removal from aqueous solution by adsorption. Mechanistic and regeneration analysis. Environ. Technol. Innov. 24, 102060 https://doi.org/10.1016/j.eti.2021.102060.

Guo, Y., Rockstraw, D.A., 2006. Physical and chemical properties of carbons synthesized from xylan, cellulose, and Kraft lignin by H3PO4 activation. Carbon 44, 1464–1475. https://doi.org/10.1016/j.carbon.2005.12.002.

Ho, Y.S., Ng, J.C.Y., McKay, G., 2000. Kinetics of pollutant sorption by biosorbents: review. Sep. Purif. Methods 29, 189–232. https://doi.org/10.1002/chin.200147289.

Hu, Q., Pang, S., Wang, D., 2021. In-depth insights into mathematical characteristics, selection criteria and common mistakes of adsorption kinetic models: a critical review. Sep. Purif. Rev. 1–19. https://doi.org/10.1080/15422119.2021.1922444.
Jackowski, M., Niedźwiecki, Ł., Jagiełło, K., Uchańska, O., Trusek, A., 2020. Brewer's spent grains—valuable beer industry by-product. Biomolecules 10, 1–18. https://doi.org/10.3390/biom10121669.
Jaria, G., Silva, C.P., Oliveira, J.A.B.P., Santos, S.M., Gil, M.V., Otero, M., Calisto, V., Esteves, V.I., 2018. Production of highly efficient activated carbons from industrial wastes for the removal of pharmaceuticals from water-A full factorial design. J. Hazard. Mater. 0–1. https://doi.org/10.1016/j.jhazmat.2018.02.053.
Kim, S.H., Shon, H.K., Ngo, H.H., 2010. Adsorption characteristics of antibiotics trimethoprim on powdered and granular activated carbon. J. Ind. Eng. Chem. 16, 344–349. https://doi.org/10.1016/j.jiec.2009.09.061.
Kovalakova, P., Cizmas, L., McDonald, T.J., Marsalek, B., Feng, M., Sharma, V.K., 2020. Occurrence and toxicity of antibiotics in the aquatic environment: a review. Chemosphere 251, 126351. https://doi.org/10.1016/j.chemosphere.2020.126351.
Lagergren, 1898. Zur theorie der sogenannten adsorption geloster stoffe. K. Sven. 24, 1–39.
Langmuir, I., 1918. The adsorption of gases on plane surfaces of glass, mica and platinum. J. Am. Chem. Soc. 40, 1361–1403. https://doi.org/10.1021/ja02242a004.
Lee, M.S., Park, M., Kim, H.Y., Park, S.J., 2016. Effects of microporosity and surface chemistry on separation performances of n-containing pitch-based activated carbons for CO_2/N2 binary mixture. Sci. Rep. 6, 1–11. https://doi.org/10.1038/srep23224.
Lee, S.Y., Park, S.J., 2010. Effect of temperature on activated carbon nanotubes for hydrogen storage behaviors. Int. J. Hydrog. Energy 35, 6757–6762. https://doi.org/10.1016/j.ijhydene.2010.03.114.
Li, H., Zheng, F., Wang, J., Zhou, J., Huang, X., Chen, L., Hu, P., Gao, J. ming, Zhen, Q., Bashir, S., Liu, J.L., 2020. Facile preparation of zeolite-activated carbon composite from coal gangue with enhanced adsorption performance. Chem. Eng. J. 390, 124513 https://doi.org/10.1016/j.cej.2020.124513.
Li, M. Fang, Liu, Y. Guo, Zeng, G. Ming, Liu, N., Liu, S. Bo, 2019. Graphene and graphene-based nanocomposites used for antibiotics removal in water treatment: a review. Chemosphere 226, 360–380. https://doi.org/10.1016/j.chemosphere.2019.03.117.
Lillo-Ródenas, M.A., Marco-Lozar, J.P., Cazorla-Amorós, D., Linares-Solano, A., 2007. Activated carbons prepared by pyrolysis of mixtures of carbon precursor/alkaline hydroxide. J. Anal. Appl. Pyrolysis 80, 166–174. https://doi.org/10.1016/j.jaap.2007.01.014.
Lingamdinne, L.P., Choi, Y.L., Kim, I.S., Yang, J.K., Koduru, J.R., Chang, Y.Y., 2017. Preparation and characterization of porous reduced graphene oxide based inverse spinel nickel ferrite nanocomposite for adsorption removal of radionuclides. J. Hazard. Mater. 326, 145–156. https://doi.org/10.1016/j.jhazmat.2016.12.035.
Liu, H., Zhang, J., Bao, N., Cheng, C., Ren, L., Zhang, C., 2012. Textural properties and surface chemistry of lotus stalk-derived activated carbons prepared using different phosphorus oxyacids: dasorption of trimethoprim. J. Hazard. Mater. 235–236, 367–375. https://doi.org/10.1016/j.jhazmat.2012.08.015.
Liu, H., Zhang, J., Ngo, H.H., Guo, W., Wu, H., Guo, Z., Cheng, C., Zhang, C., 2015. Effect on physical and chemical characteristics of activated carbon on adsorption of trimethoprim: mechanisms study. RSC Adv. 5, 85187–85195. https://doi.org/10.1039/c5ra17968h.
Malakootian, M., Yaseri, M., Faraji, M., 2019. Removal of antibiotics from aqueous solutions by nanoparticles: a systematic review and meta-analysis. Environ. Sci. Pollut. Res. 26, 8444–8458. https://doi.org/10.1007/s11356-019-04227-w.
Miller, J., & Miller, J.C., 2005. Statistics and chemometrics for analytical chemistry.
Moulefera, I., García-Mateos, F.J., Benyoucef, A., Rosas, J.M., Rodríguez-Mirasol, J., Cordero, T., 2020. Effect of co-solution of carbon precursor and activating agent on the textural properties of highly porous activated carbon obtained by chemical activation of lignin With H3PO4. Front. Mater. 7, 1–14. https://doi.org/10.3389/fmats.2020.00153.
Mussatto, S.I., Fernandes, M., Rocha, G.J.M., Órfão, J.J.M., Teixeira, J.A., Roberto, I.C., 2010. Production, characterization and application of activated carbon from Brewer's spent grain lignin. Bioresour. Technol. 101, 2450–2457. https://doi.org/10.1016/j.biortech.2009.11.025.
Nielsen, L., Biggs, M.J., Skinner, W., Bandosz, T.J., 2014. The effects of activated carbon surface features on the reactive adsorption of carbamazepine and sulfamethoxazole. Carbon 80, 419–432. https://doi.org/10.1016/j.carbon.2014.08.081.
Oliveira, G., Calisto, V., Santos, S.M., Otero, M., Esteves, V.I., 2018. Paper pulp-based adsorbents for the removal of pharmaceuticals from wastewater: a novel approach towards diversification. Sci. Total Environ. 631–632, 1018–1028. https://doi.org/10.1016/j.scitotenv.2018.03.072.
Örkün, Y., Karatepe, N., Yavuz, R., 2012. Influence of temperature and impregnation ratio of H3PO 4 on the production of activated carbon from hazelnut shell. Acta Phys. Pol. A 121, 277–280. https://doi.org/10.12693/APhysPolA.121.277.
Osman, A.I., O'Connor, E., McSpadden, G., Abu-Dahrieh, J.K., Farrell, C., Al-Muhtaseb, A.H., Harrison, J., Rooney, D.W., 2020. Upcycling brewer's spent grain waste into activated carbon and carbon nanotubes for energy and other applications via two-stage activation. J. Chem. Technol. Biotechnol. 95, 183–195. https://doi.org/10.1002/jctb.6220.
Premarathna, K.S.D., Rajapaksha, A.U., Adassoriya, N., Sarkar, B., Sirimuthu, N.M.S., Cooray, A., Ok, Y.S., Vithanage, M., 2019. Clay-biochar composites for sorptive removal of tetracycline antibiotic in aqueous media. J. Environ. Manag. 238, 315–322. https://doi.org/10.1016/j.jenvman.2019.02.069.
Rodrigues, A.E., Silva, C.M., 2016. What's wrong with Lagergreen pseudo first order model for adsorption kinetics? Chem. Eng. J. 306, 1138–1142. https://doi.org/10.1016/j.cej.2016.08.055.
Rudzinski, W., Plazinski, W., 2007. Studies of the kinetics of solute adsorption at solid/solution interfaces: on the possibility of distinguishing between the diffusional and the surface reaction kinetic models by studying the pseudo-first-order kinetics. J. Phys. Chem. C 111, 15100–15110. https://doi.org/10.1021/jp073249c.
Saucier, C., Adebayo, M.A., Lima, E.C., Cataluña, R., Thue, P.S., Prola, L.D.T., Puchana-Rosero, M.J., Machado, F.M., Pavan, F.A., Dotto, G.L., 2015. Microwave-assisted activated carbon from cocoa shell as adsorbent for removal of sodium diclofenac and nimesulide from aqueous effluents. J. Hazard. Mater. 289, 18–27. https://doi.org/10.1016/j.jhazmat.2015.02.026.
Shang, J.G., Kong, X.R., He, L.L., Li, W.H., Liao, Q.J.H., 2016. Low-cost biochar derived from herbal residue: characterization and application for ciprofloxacin adsorption. Int. J. Environ. Sci. Technol. 13, 2449–2458. https://doi.org/10.1007/s13762-016-1075-3.
Silva, C.P., Jaria, G., Otero, M., Esteves, V.I., Calisto, V., 2019. Adsorption of pharmaceuticals from biologically treated municipal wastewater using paper mill sludge-based activated carbon. Environ. Sci. Pollut. Res. 26, 13173–13184. https://doi.org/10.1007/s11356-019-04823-w.
Silva, C.P., Jaria, G., Otero, M., Esteves, V.I., Calisto, V., 2018. Waste-based alternative adsorbents for the remediation of pharmaceutical contaminated waters: has a step forward already been taken? Bioresour. Technol. 250, 888–901. https://doi.org/10.1016/j.biortech.2017.11.102.
Sousa, A.F.C., Gil, M.V., Calisto, V., 2020. Upcycling spent brewery grains through the production of carbon adsorbents—application to the removal of carbamazepine from water. Environ. Sci. Pollut. Res. 27, 36463–36475. https://doi.org/10.1007/s11356-020-09543-0.
Sousa, É., Rocha, L., Jaria, G., Gil, M.V., Otero, M., Esteves, V.I., Calisto, V., 2021. Optimizing microwave-assisted production of waste-based activated carbons for the removal of antibiotics from water. Sci. Total Environ. 752, 141662 https://doi.org/10.1016/j.scitotenv.2020.141662.
Stoeckli, F., Ballerini, L., 1991. Evolution of microporosity during activation of carbon. Fuel 70, 557–559. https://doi.org/10.1016/0016-2361(91)90036-A.
Sun, Y., Yue, Q., Gao, B., Gao, Y., Xu, X., Li, Q., Wang, Y., 2014. Adsorption and cosorption of ciprofloxacin and Ni(II) on activated carbon-mechanism study. J. Taiwan Inst. Chem. Eng. 45, 681–688. https://doi.org/10.1016/j.jtice.2013.05.013.
Teixeira, S., Delerue-Matos, C., Santos, L., 2019. Application of experimental design methodology to optimize antibiotics removal by walnut shell based activated carbon. Sci. Total Environ. 646, 168–176. https://doi.org/10.1016/j.scitotenv.2018.07.204.
Tsukamoto, T., Yasuma, M., Yamamoto, A., Hirayama, K., Kihou, T., Kodama, S., Inoue, Y., 2009. Evaluation of sulfobetaine-type polymer resin as an SPE adsorbent in the analysis of trace tetracycline antibiotics in honey. J. Sep. Sci. 32, 3591–3595. https://doi.org/10.1002/jssc.200900520.
Turk Sekulic, M., Boskovic, N., Slavkovic, A., Garunovic, J., Kolakovic, S., Pap, S., 2019. Surface functionalised adsorbent for emerging pharmaceutical removal: Adsorption performance and mechanisms. Process Saf. Environ. Prot. 125, 50–63. https://doi.org/10.1016/j.psep.2019.03.007.
Uivarosi, V., 2013. Metal complexes of quinolone antibiotics and their applications: an update. Molecules 18, 11153–11197. https://doi.org/10.3390/molecules180911153.
Velo-Gala, I., López-Peñalver, J.J., Sánchez-Polo, M., Rivera-Utrilla, J., 2014. Surface modifications of activated carbon by gamma irradiation. Carbon 67, 236–249. https://doi.org/10.1016/j.carbon.2013.09.087.
Wang, Y.X., Ngo, H.H., Guo, W.S., 2015. Preparation of a specific bamboo based activated carbon and its application for ciprofloxacin removal. Sci. Total Environ. 533, 32–39. https://doi.org/10.1016/j.scitotenv.2015.06.087.
Wu, X., Huang, M., Zhou, T., Mao, J., 2016. Recognizing removal of norfloxacin by novel magnetic molecular imprinted chitosan/γ-Fe2O3 composites: Selective adsorption mechanisms, practical application and regeneration. Sep. Purif. Technol. 165, 92–100. https://doi.org/10.1016/j.seppur.2016.03.041.
Zbair, M., Ait Ahsaine, H., Anfar, Z., 2018. Porous carbon by microwave assisted pyrolysis: n effectiave and low-cost adsorbent for sulfamethoxazole adsorption and optimization using response surface methodology. J. Clean. Prod. 202, 571–581. https://doi.org/10.1016/j.jclepro.2018.08.155.
Zhang, B., Han, X., Gu, P., Fang, S., Bai, J., 2017. Response surface methodology approach for optimization of ciprofloxacin adsorption using activated carbon derived from the residue of desilicated rice husk. J. Mol. Liq. 238, 316–325. https://doi.org/10.1016/j.molliq.2017.04.022.